

7-1-2011

Emerging Solar Cell Technology: Advances in Solid-state Polymer Hybrid Dye-sensitized Solar Cells

Andrew de Jong
Pomona College

Recommended Citation

de Jong, Andrew, "Emerging Solar Cell Technology: Advances in Solid-state Polymer Hybrid Dye-sensitized Solar Cells" (2011). *Environmental Analysis Program Mellon Student Summer Research Reports*. Paper 1.
http://scholarship.claremont.edu/eap_ea_mellonreports/1

This Undergraduate Research Project is brought to you for free and open access by the Environmental Analysis Program at the Claremont Colleges at Scholarship @ Claremont. It has been accepted for inclusion in Environmental Analysis Program Mellon Student Summer Research Reports by an authorized administrator of Scholarship @ Claremont. For more information, please contact scholarship@cuc.claremont.edu.

Emerging Solar Cell Technology: Advances in Solid-state Polymer Hybrid Dye-sensitized Solar Cells

Andrew de Jong

Mellon Research Project, Summer 2011



Credit: Snaith, Schmidt-Mende, 2010 [9]

Summary and Abstract

My project this summer took place in the lab of Dr. Henry J. Snaith, head of the Optoelectronic and Photovoltaic Device Group at Oxford University, a sub-group of Condensed Matter Physics in the Oxford Physics Department. I worked for ten weeks on solid-state dye-sensitized solar cells that incorporated the polymer hole-transporter poly(3-hexylthiophene) (P3HT) and a number of different dyes. The larger goal of the project is to extend solid-state solar cells' photoresponse by taking advantage of a favorable energy-transfer mechanism between P3HT and dyes that absorb close to the onset of the infrared spectrum. As the system is not fully understood—further steps must be taken to develop a working predictive model of the dye-sensitized solar cell—the experimental approach tends to be more or less in the realm of try-lots-of-things-out-and-see-if-they-work. Therefore, I spent large amounts of time in the lab overwhelmed by the prospect of a nearly infinite number of permutations of parameters to test. The technology has much promise in large part because so much has yet to be tried, and one of the most important things I learned was the necessity of developing effective heuristics for narrowing down the choices of what to pursue. Here, I report some of the more relevant experiments and findings that fit well within the broader (and rapidly expanding) context of dye-sensitized cell research.

Introduction

Transition to sustainable and alternative energy sources.

The imperatives for a rapid transition from fossil fuel-based energy production to renewable and sustainable methods are by now widely recognized and accepted. In 2007, worldwide energy consumption was 458×10^{18} joules, equivalent to the consumption rate of 16.2 terawatts (TW, one TW is 10^{12} joules per second) [1]. Energy demand is expected to increase by 50% by 2035 as the population continues to grow to around 9 billion in 2050 [2]. The projected acceleration of energy consumption comes not only from Earth's new inhabitants but also from over 3 billion people in the developing world. In order to meet this demand major advances in technology and production scale are required in all renewable energy resource sectors.

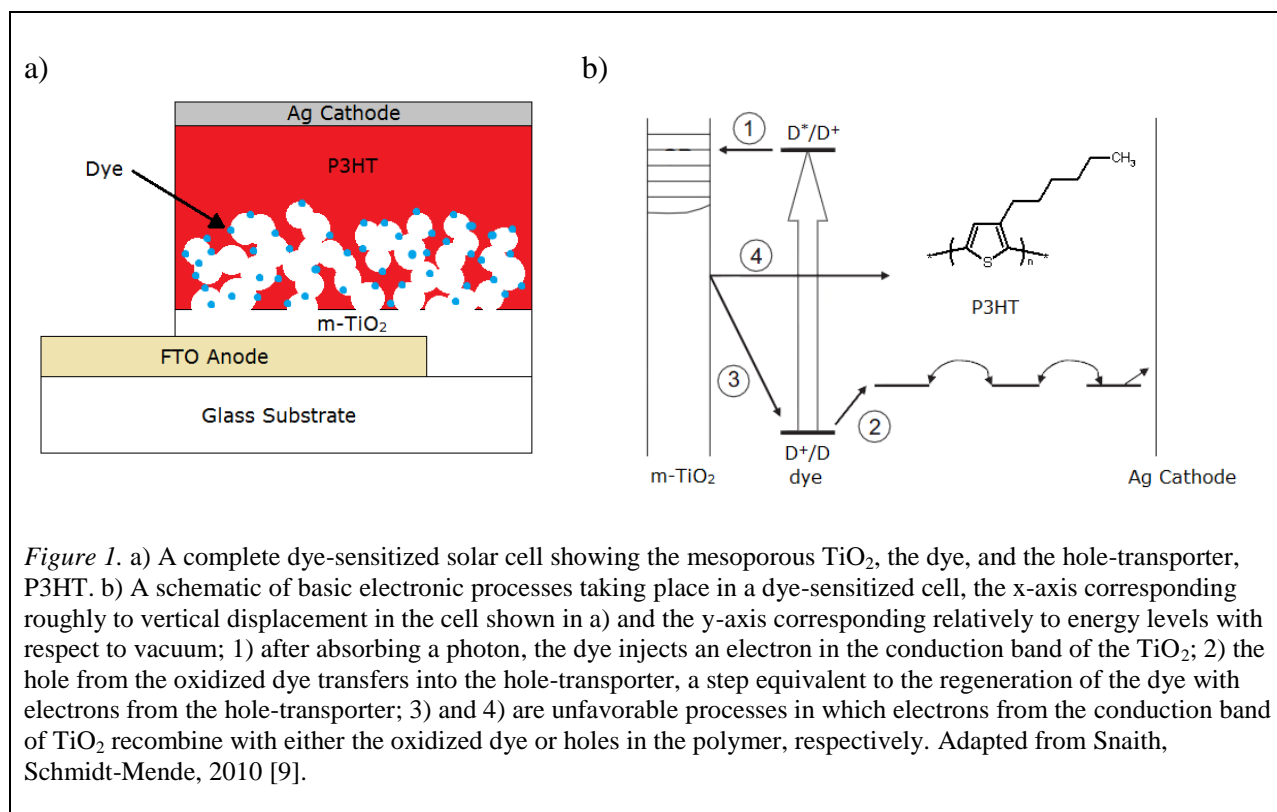
Capturing the energy emitted by the sun, which has illuminated the solar system day after day for about 5 billion years at a rate of 1.7×10^5 TW or 1.7×10^{17} joules per second, holds easily graspable potential for meeting a large portion of anticipated energy demand in the future [3]. Solar energy production has increased from 201 megawatts (MW) in 1999 to 10,680 MW in 2009, nearly all of which has come from crystalline silicon arrays [4]. In 2009, 80% of photovoltaic production was from crystalline silicon cells; however, with fluctuations in the cost and manufacturing of polycrystalline silicon, the newer and cheaper "thin-film photovoltaics" expect even more rapid growth in the next decade [5]. Current thin-film photovoltaic production consists of copper-indium-gallium-selenide (CIGS) cells, cadmium telluride (CdTe) cells, and amorphous silicon (a-Si) cells, though growth for several of the technologies that require rare earth metals, telluride, for example, is limited due to these metals' scarcity in Earth's crust. Several new photovoltaic technologies, such as dye-sensitized cells, are in the preliminary stages of commercialization, and much current research and funding is being directed towards the practicalities of industrial scale-up.

Dye-sensitized solar cells.

The dye-sensitized solar cell is a herald of the newest generation of solar cell technology with a current lab efficiency benchmark of around 11% [6]. Considered a thin-film technology, cells, built on top of a glass substrate, range from 1 to 15 μm in thickness. Constructed from organic or plentiful inorganic material, these devices can be manufactured by solution- or reel-to-reel-processing methods, promising very cheap, low energy production. In addition, they can be made with a large range of materials, giving unparalleled flexibility in the ability to fine-tune electronic or aesthetic properties. They also perform relatively better under diffuse light conditions and at higher temperatures than other photovoltaic technology. Rather than being incorporated into large array of solar power plants, the biggest market for the dye-sensitized cell will most likely be in buildings and construction [7]. The tunability of the dye color and its transparency—freedoms that no existing solar technology holds yet—gives these cells serious

potential at being implemented into windows for the dual purpose of tinting and power generation.

Dye cells have three major parts, a porous layer of titanium dioxide (TiO_2) nanoparticles, a monolayer of dye that covers the particles, and a “hole-transporter” that infiltrates the pores within the TiO_2 layer. Titanium dioxide has been used for several decades as a white powder pigment and is one of the fifty most-produced compounds worldwide, having been incorporated into food, plastics, paper, paint, and cosmetics [8]. A porous layer, or more specifically a “mesoporous” layer, because the particles’ sizes range from 10 to 50 nm, is needed within the structure to provide a large surface area onto which the dye will adsorb. The dyes in the highest efficiency cells are based on ruthenium, another rare earth metal, though considerable effort is being made to transition to organic dyes such as porphyrin dyes, the class chlorophyll dyes are in, or “donor- π -acceptor” dyes, named for the electronic functionality of the molecule’s components. The hole-transporting material (HTM) is made of an iodide/triiodide liquid electrolyte in the highest performing cells, though steps are being made to incorporate solid HTMs instead, due to the thermal instability of liquids and the problems posed for sealing by thermal expansion. Both polymers and small molecules are being examined for their use in solid-state dye-sensitized solar cells. 2,2',7,7'-tetrakis-(N,N-di-pmethoxyphenylamine)9,9'-spiro-bifluorene (spiro-OMeTAD) is the most widely used solid-state hole conductor, though in this study the conducting polymer poly(3-hexylthiophene) (P3HT) is used.



The dye-sensitized cell begins to perform when a dye molecule attached to the titania surface absorbs a photon. The molecule becomes excited and an electron makes an energetic transition from the ground-state highest occupied molecular orbital (HOMO) to an excited state, the lowest unoccupied molecular orbital (LUMO). Energetically, the LUMO of the dye needs to be higher than the conduction band of the TiO_2 such that injection from the dye to the titania is favored. Though TiO_2 is an insulator and not typically thought of as a material well-suited to conducting charge, the large band gap allows electrons to flow relatively freely within its conduction band. The electrons flow through the mesoporous titania nanostructure, to the fluorine-doped tin dioxide anode and out of the cell. Meanwhile, the dye cation is regenerated by electrons from the hole-transport material, P3HT, and the hole diffuses through this layer to the silver cathode, completing the circuit. Recombination processes occur when electrons and holes meet and release energy, reducing the cell's efficiency. A diagram of a complete dye-sensitized cell and a scheme of electronic processes occurring in the cell are presented in Figure 1.

Extending photoresponse through complementary interaction of near-IR dyes and the polymer hole-transport material, P3HT.

As stated above, the purpose of this project in the Snaith group is to extend the photoresponse of solid-state dye-sensitized cells to increase current generation. A new direction has been taken recently with the incorporation of P3HT into solid-state cells in place of spiro-OMeTAD because P3HT can plausibly act as both a hole-transporter and a light absorber—P3HT is red while spiro-OMeTAD is transparent. The goal is to take advantage of a resonant energy transfer (FRET) process that would be expected to occur if the absorbance spectrum of the dye correctly overlaps with the photoluminescent spectrum of the P3HT and the molecules are within several nanometers of one another. It is known that P3HT photoluminesces at around 725 nm, though the number of dyes with such a small band gap is very low, which presents a challenge to experimentation. If both the P3HT and the dye absorb light and the P3HT serves as an antenna, relaying the energy absorbed to the dye, with the dye injected the electrons into the TiO_2 mesostructure, clear panchromatic response could be reasonably attained and efficiencies for solid-state devices markedly improved.

Experimental

Assembly of dye-sensitized solar cells.

A 11 cm by 9.8 cm fluorine-doped tin oxide (FTO) pre-coated glass sheet from Pilkington was etched with zinc powder and 2M HCl to create the desired electrode pattern and washed with deionized water, soap (2% Hallmanex in water), acetone, and ethanol, then allowed to air dry. The etched glass substrate was treated to oxygen plasma etching for 10 minutes to remove all remaining organic residue. A titanium diisopropoxide bis(acetylacetonate) (Ti-ACAC) precursor

was mixed in a 1:10 ratio with anhydrous ethanol and sprayed uniformly in air over the glass substrate, which was heated to 500 °C, to form a 100 nm compact layer of TiO₂.

To deposit a 1 μm mesoporous TiO₂ layer, 1 g of TiO₂ nanoparticle paste (from Dyesol, 20 nm diameter particle size) was mixed with 0.7 mL of anhydrous terpineol, then stirred and ultrasonicated to ensure complete mixing. The paste was screenprinted onto the glass substrate using a 120 mesh-count screen to create a wet TiO₂ film. The substrate was heated to 550 °C over 90 minutes, permitting the solvents in the deposited paste to evaporate, and held at the maximum temperature for 30 minutes to burn off the cellulose binder in the paste and sinter the nanoparticles together. After complete cooling, the substrates were cut into individual 1.4 cm by 1.4 cm devices and soaked in a 15M TiCl₄ solution in water at 70 °C for one hour. The cells were rinsed with deionized water and ethanol and dried in air before being heated once again to 550 °C for 45 minutes in air to complete the resintering process. Once baking was complete, the cells were cooled to 70 °C to avoid water accumulation on the mesoporous TiO₂ surface before dye-loading.

A number of dyes were prepared for these experiments. The TT1 dye solution was 0.05 mM in anhydrous ethanol, with varying concentrations of chenodeoxycholic acid (CDCA) added to prevent dye aggregation on the TiO₂ surface. D102, P565, P587, P594, and P778 dye solutions were 0.5 mM in a 1:1 by volume mixture of anhydrous acetonitrile and *tert*-butanol. The devices were transferred from a 70 °C hotplate directly into dye solution, the beakers covered and sealed to prevent evaporation of solvent. Dyeing time ranged from 1 to 4 hours depending on the experiment, but once fully dyed the cells were rinsed in their respective dye solvents and dried with clean compressed air before spin-coating.

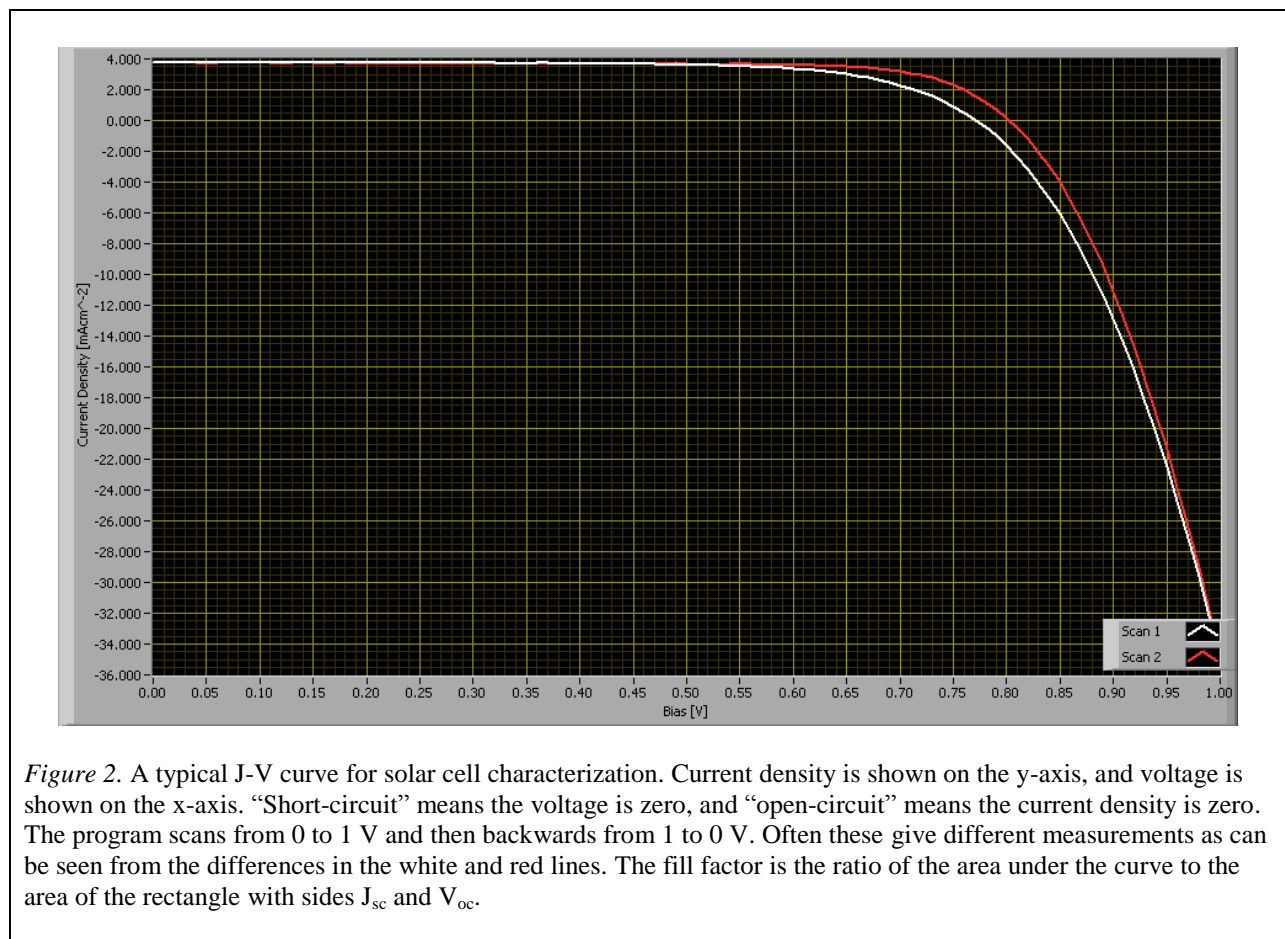
Regioregular poly(3-hexylthiophene) (P3HT) polymer from Rieke Metals, Inc. was dissolved in anhydrous chlorobenzene at 3 wt% concentration in preparation for spin-coating. Additionally, solutions of additives were made for spin-coating: for solutions with both the Li-TFSI and *t*-bp additives, solutions were made with 35 μL of a 170 mg mL⁻¹ Li-TFSI/ACN stock solution and 7 μL of anhydrous *t*-bp solvent in 385 μL of anhydrous ACN (for solutions with only Li-TFSI, the *t*-bp solvent simply was not added). The spin-coating process was carried out for 60 seconds at 1000 RPM beginning with an acceleration of 500 RPM/s. Twenty-five μL of either additive or polymer solution was pipetted uniformly over the dye-adsorbed device and left to wet the surface for 30 seconds before commencing spin-coating. If the experiment called for additives, the Li-TFSI/*t*-bp/ACN solution was always spun onto the device prior to P3HT solution.

Silver electrode deposition 150 nm thick was carried out in a thermal evaporator under high vacuum (10⁻⁶ mbar), to give cells with active areas of 0.09 cm². For solar simulator and spectral response experiments, the cells were masked properly around the active area to ensure the accuracy of measurements.

Device characterization instruments and measurements.

Solar Simulator

The solar simulator measures performance characteristics of complete solar cells. By illuminating the devices through the glass substrate with a 100 W AM 1.5 G lamp, used to reproduce the solar spectrum, short-circuit photocurrent density (J_{sc}) measured as milliamps per square centimeter (mA cm^{-2}), open-circuit photovoltage (V_{oc}) measured in volts (V), and fill factor (FF) expressed as a unitless number between 0 and 1 can be obtained. The product of these measured parameters is power conversion efficiency (%). A “J-V curve”, the graph off of which these parameters are read, is shown in Figure 2.



Spectral Response

The spectral response of a solar cell refers to its capacity at a certain wavelength to convert incident photons to current. This is expressed as the “external quantum efficiency” (EQE) or the incident photon-to-electron conversion efficiency (IPCE). Measurements are taken by

illuminating the cell with monochromatic light at short circuit, recording the photocurrent density produced, and dividing this by the photon flux. Coupled with the unique absorbance characteristics of separate materials used to construct the solar cell, such as the dye or hole-transporter, much can be inferred regarding the precise power-producing capabilities of the device's photoactive components.

Absorbance and Photoluminescence measurements

Absorbance and photoluminescence spectra of photoactive materials provide a wealth of information regarding the materials' quantum properties. The magnitude of energetic transitions within dyes and, if measured at very short timescales (femto- to picosecond), kinetic data concerning movements of electrons and holes at material interfaces can be produced from analysis of these characteristics. Measurements of nearly whole devices can be taken, from which charge- and energy- transfer mechanisms can be inferred. Most important for the purposes of this study has been the link between spectral response data and absorbance spectra.

Results and Discussion

Effect of ions and Lewis bases as additives in TT1/P3HT cells: 4-tert-butyl pyridine (t-bp) and lithium bis(trifluoromethylsulfonyl)imide salt (Li-TFSI).

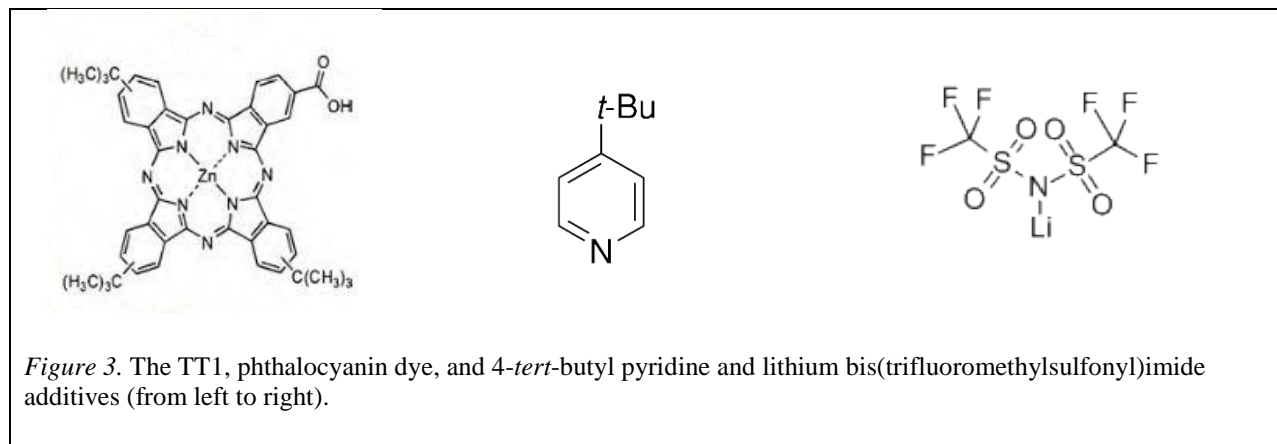


Figure 3. The TT1, phthalocyanin dye, and 4-*tert*-butyl pyridine and lithium bis(trifluoromethylsulfonyl)imide additives (from left to right).

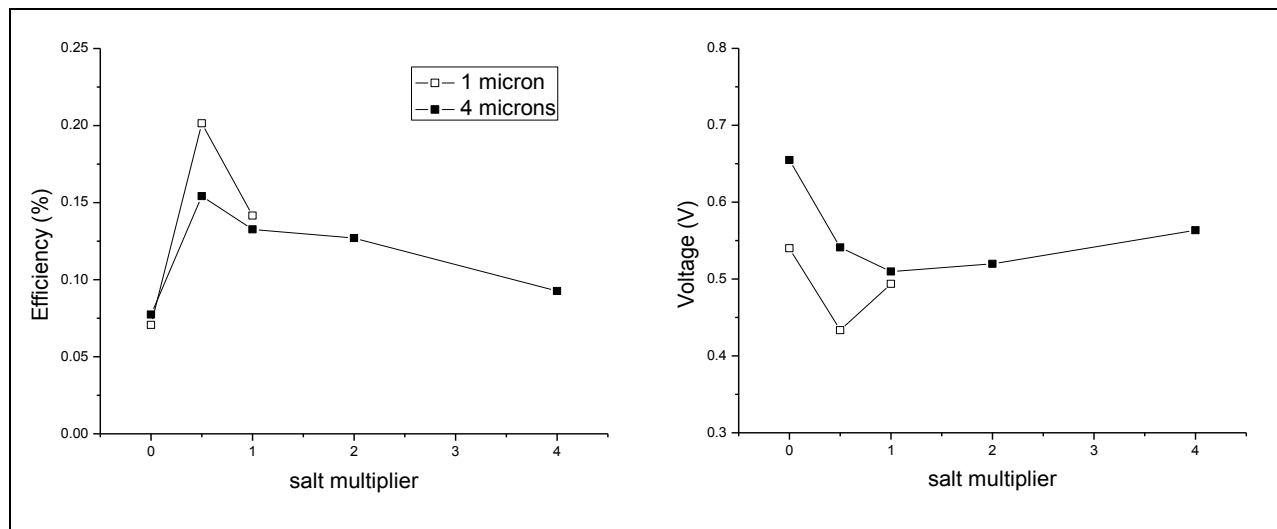
Ionic additives are known to play a large role in tuning local electronic properties of interfaces within dye-sensitized cells, though the exact effect and method of incorporation seems to change from system to system. In P3HT cells, Li-TFSI is thought to catalyze a reaction between P3HT and oxygen that results in oxygen vacancies and p-doping of the polymer, and increases its crystallinity which improves hole mobilities. In addition lithium, which possesses a large charge density, induces an effect on the titania surface similar to protons, which decrease surface potential by 59 meV per pH unit, markedly decreasing the open-circuit voltage of solar cells.

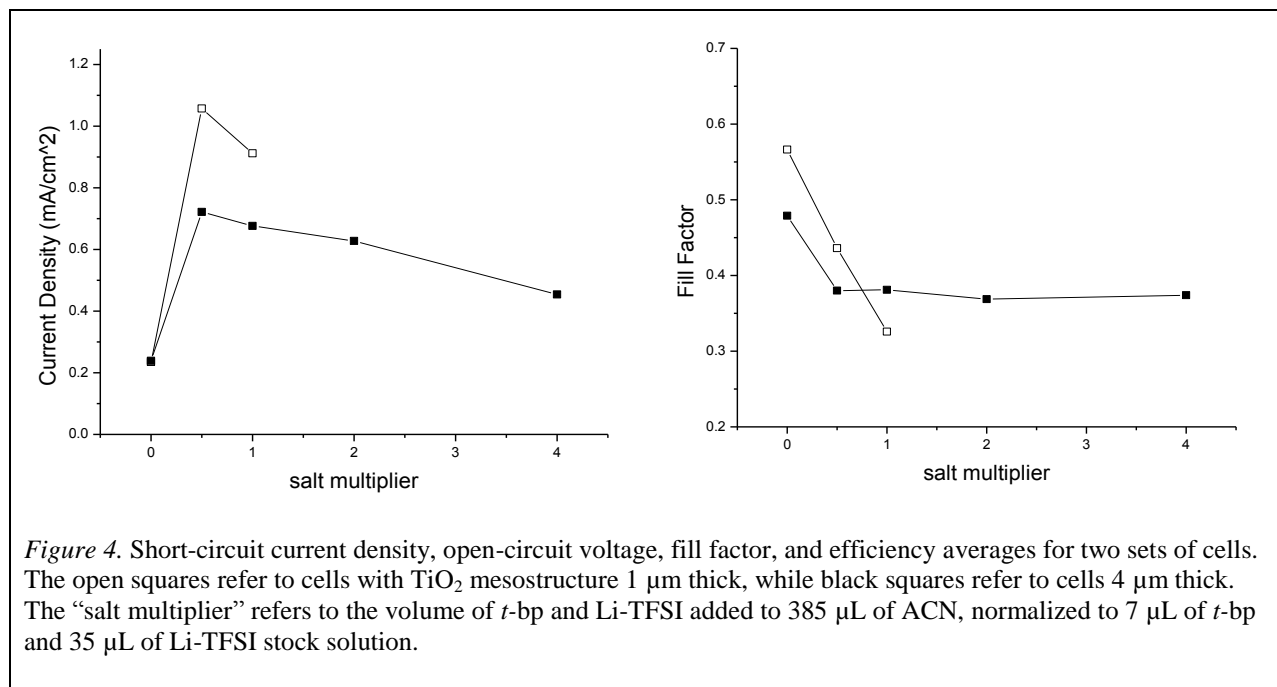
However, the efficiency lost by this voltage reduction is typically made up by a major increase in short-circuit current density. The presence of the localized positive cation in the titania-dye matrix creates an electric field pointing towards the TiO_2 surface. When the dye absorbs a photon, the additional electron density is shuttled favorably towards the titania surface and injection into its conduction band. 4-*Tert*-butyl pyridine on the other hand, a Lewis base, serves to attract any protons on the TiO_2 surface and shelter them, effectively recovering the voltage loss.

Devices were made with the intention of achieving an optimal concentration of Li-TFSI and *t*-bp for the TT1/P3HT system. Experimentally, an additive solution is made with the volumes outlined above and a small amount is spin-coated on the cell after dyeing but before P3HT deposition. This coats the pores of the titania and has been shown to aid pore infiltration and charge extraction of P3HT.

It was found that though the effect of the additive content is noticeable on device performance, the effect of the mesostructure thickness is large as well. The screen-printing step in which the titania paste is applied to the prepared glass substrate is very sensitive to both the concentration of TiO_2 nanoparticles in the paste and the mesh count of the screen. As such, for a beginner, applying a layer of the same thickness on subsequent sheets is quite difficult but has been found to have a large impact on device performance. Thickness dependence is thought to be an issue due to insufficient pore-filling of the P3HT into the TiO_2 structure which inhibits charge extraction to the electrode by the polymer.

Figure 4 displays the solar simulator data for these batches of cells with different thicknesses and additive contents. Thinner devices perform better than thicker ones do, and devices with half the additive content dissolved in ACN perform the best in both thicknesses. It can be seen clearly how voltage and current density vary inversely due to numerous electronic and energetic trade-offs.





Preliminary examination of oxygen-doping effects on TT1/P3HT cells: Epoxy sealing in air and under N₂.

Recent reports suggest that the high hole conductivity of P3HT is due to p-doping by atmospheric oxygen, a reaction also catalyzed by Li-TFSI. The hole-transporter function of the P3HT seems to be in direct competition with the desired energy transfer mechanism via FRET from P3HT to the dye molecule. By eliminating oxygen in the system and comparing this to a control, the effects of oxygen (or something else in the ambient atmosphere) on P3HT can become better known. In spectral response experiments, one would expect to see a greater contribution from P3HT and a slight decrease in TT1, as the energy transfer mechanism from P3HT to TT1 is bolstered by the decrease in p-doping.

For these cells, all steps were carried out under air except sealing. The cells to be sealed in the glovebox were placed under the N₂ atmosphere two days before sealing to let oxygen and water vapor diffuse out. Care was taken to cover the active area entirely and make contact all the way around this area between the epoxy and the glass.

Shown in Figure 5 are the external quantum efficiencies of the working cells overlaying absorbance spectra for the device’s components. It is important to note that there at least exists some contribution toward photocurrent from the P3HT, as indicated by the hump in both spectra around 520 nm. However, no trend can be concluded between additive concentrations or sealing conditions. The fluctuations are most likely attributable to device-specific inconsistencies rather than to the experimental variable.

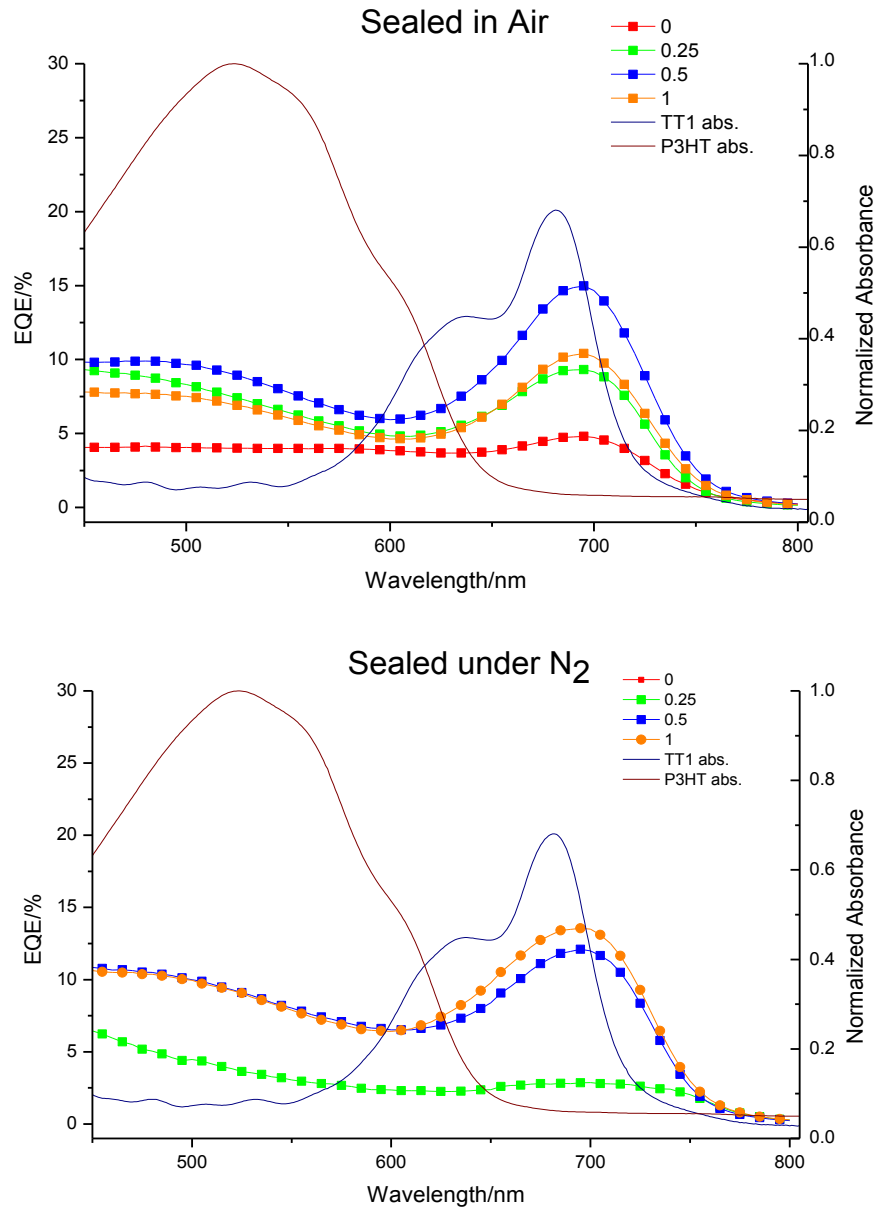
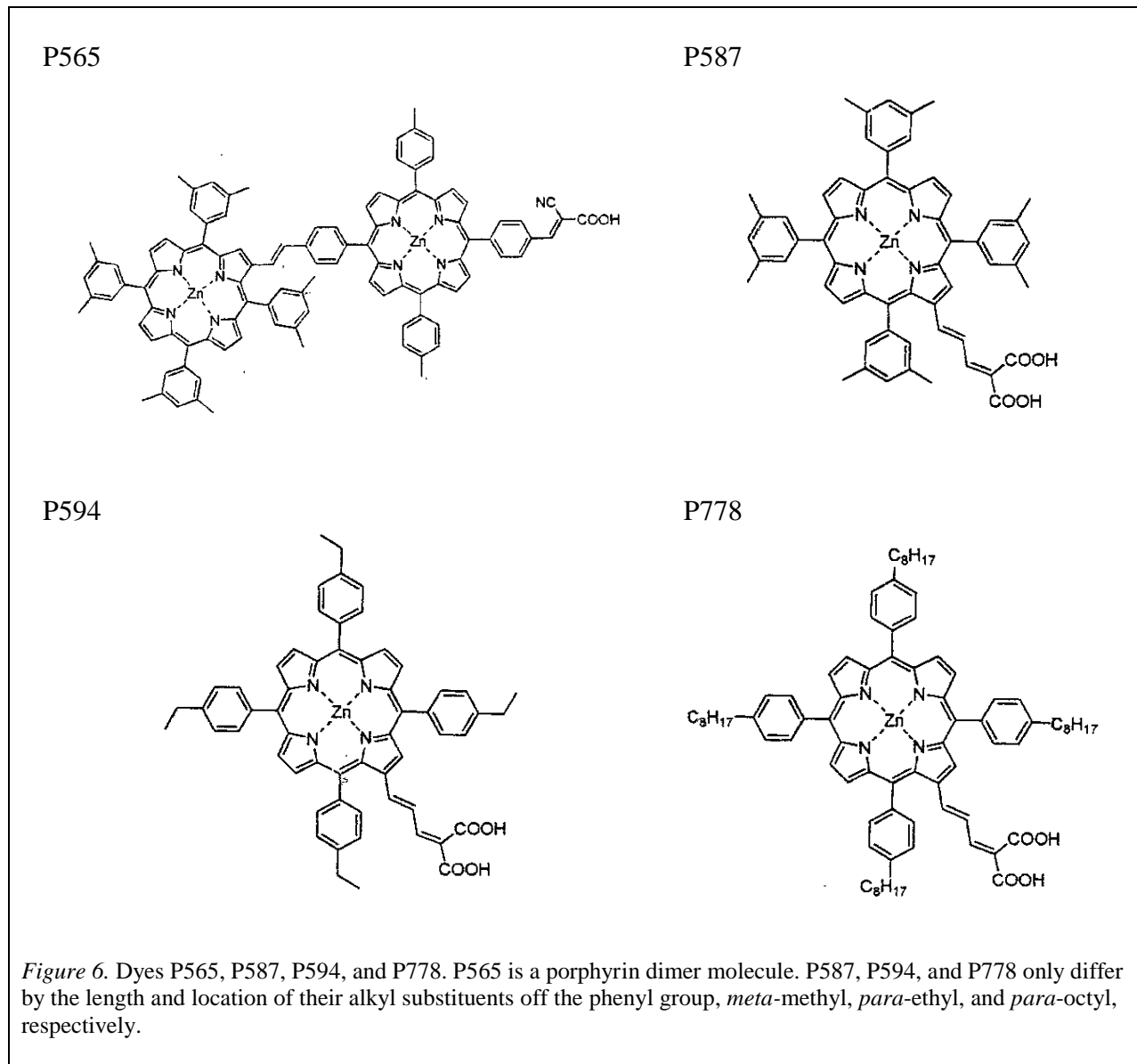


Figure 5. Spectral response of TT1/P3HT devices sealed with epoxy in air or nitrogen-rich environments made with four different concentrations of Li-TFSI/t-bp additives. The “1” label refers to the typical additive volumes of 7 μL t-bp and 35 μL Li-TFSI in 385 μL ACN; the multiples refer to changes in the volumes of t-bp and Li-TFSI only. These EQE spectra are superimposed over absorbance spectra of TT1 and P3HT measured on TiO_2 substrates.

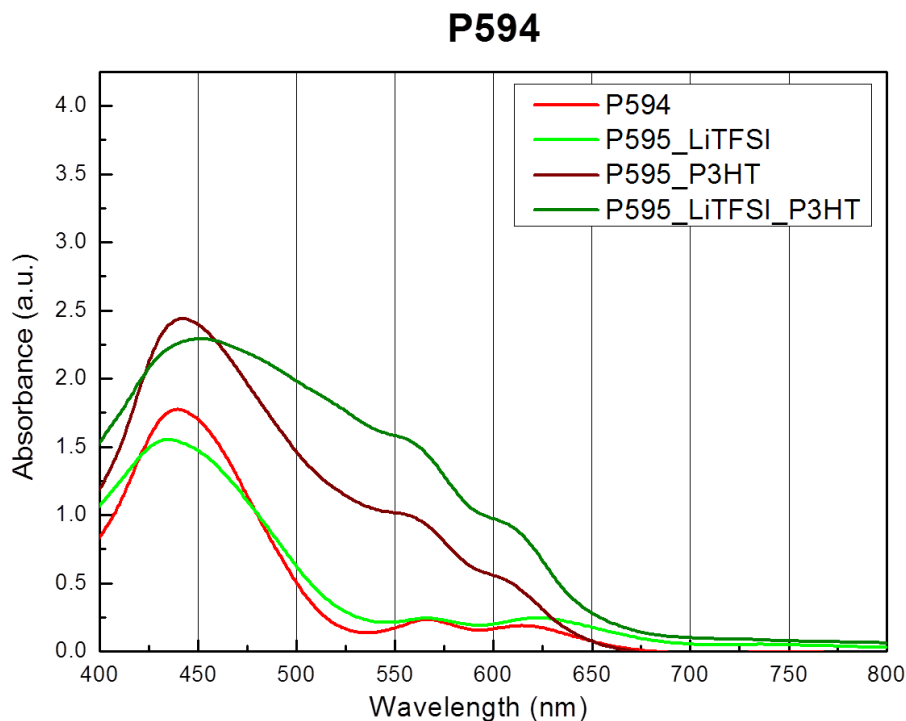
The effect of Li-TFSI on porphyrin dyes P565, P587, P594, and P778

Progress wasn't being made with TT1 so a new series of dyes was started on, these based on the porphyrin unit as found in chlorophyll. Figure 6 shows the four dyes used in the new cells.



In order to get a sense of how they worked in devices, the dyes were used with P3HT and tested with or without the Li-TFSI additive. Interestingly enough, an explainable trend was found when comparing the length of the alkyl substituent to the effect of Li-TFSI. The alkyl groups seem to shield the dye molecule from the ionic effects of the Li-TFSI that would otherwise stabilize the excited charge transfer state of the dye molecule and increase electron injection speeds, resulting in a higher short-circuit current density. The lower open-circuit voltage in the cells is attributable

to a downward band shift of the TiO₂ band edge due to Li-TFSI intercalating into the titania matrix. This data is shown in Figure 7 along with a series of absorbance spectra for one of the dyes in various device environments. The table clearly shows the voltage decrease and current increase induced by Li-TFSI, and it can be seen that the current improvement decreases with increasing alkyl substituent length while the voltage decrease remains constant.



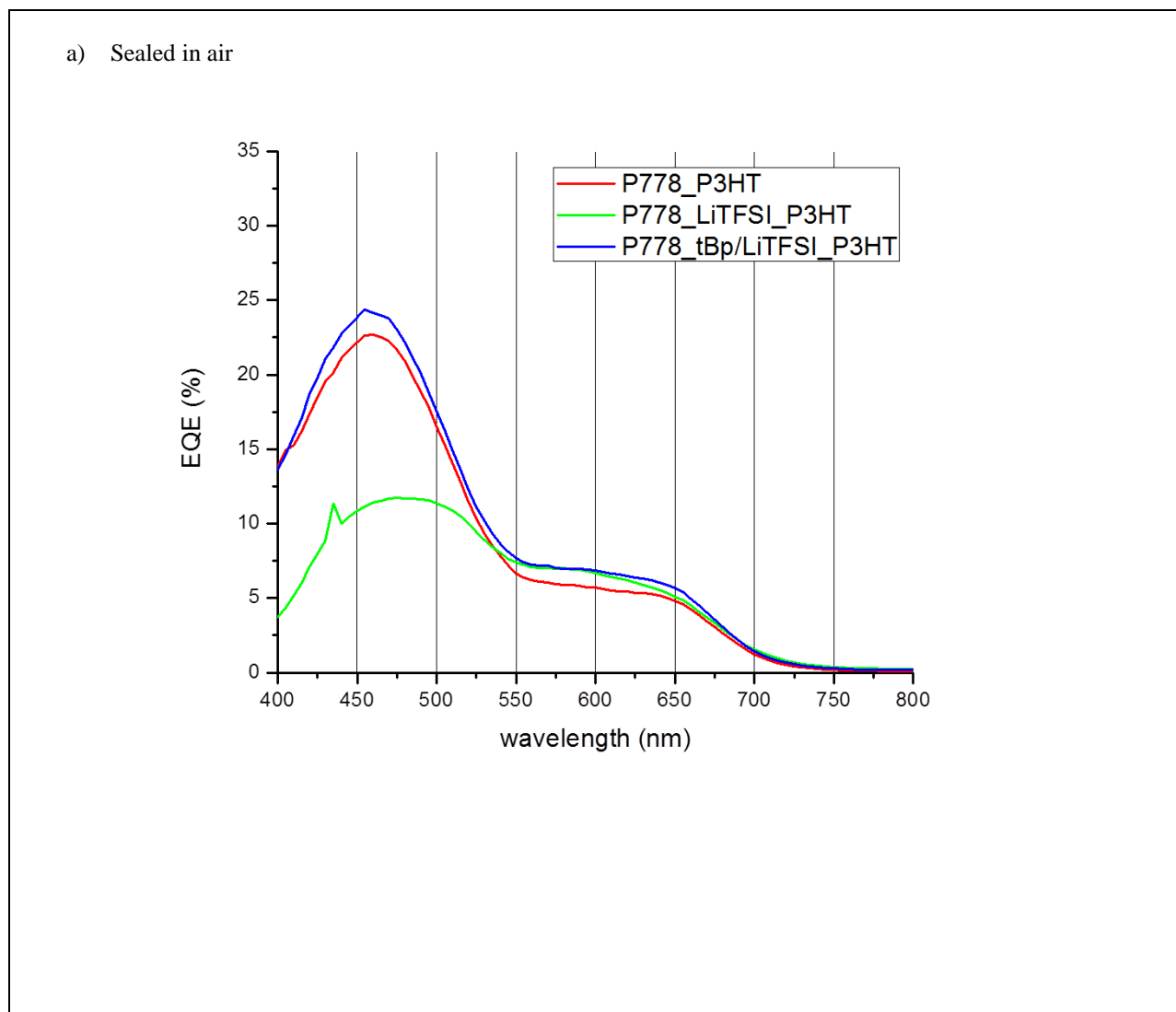
| | additives | J_{sc} (mA/cm ²) | Eff. (%) | V_{oc} (V) | FF |
|------|-------------|--------------------------------|----------|--------------|------|
| P565 | none | 0.46 | 0.13 | 0.65 | 0.41 |
| | Li-TFSI/ACN | 1.29 | 0.24 | 0.42 | 0.44 |
| P587 | none | 1.27 | 0.37 | 0.71 | 0.41 |
| | Li-TFSI/ACN | 3.68 | 0.43 | 0.45 | 0.27 |
| P594 | none | 2.36 | 0.62 | 0.73 | 0.37 |
| | Li-TFSI/ACN | 4.77 | 0.69 | 0.30 | 0.48 |
| P778 | none | 2.62 | 0.85 | 0.75 | 0.45 |
| | Li-TFSI/ACN | 2.43 | 0.39 | 0.38 | 0.41 |

Figure 7. a) Absorbance spectrum of P594 on TiO₂ with and without Li-TFSI salt and P3HT, a representative example of the other three dyes; b) table of performance characteristics for cells with and without Li-TFSI additives.

Further study of oxygen-doping on P3HT.

Because the dyes were demonstrated to function well in a P3HT device, the sealing experiments were again attempted with two new dyes, P594 and P778. This time, dyeing, spin-coating, evaporation and sealing were all carried out in the glovebox, removing any doubt that oxygen was present in the cell.

The EQE spectra presented in Figure 8 clearly indicate that different processes are taking place in each of the cells. Efficiency measurements were not collected due to known connection issues on the solar simulator between cells with epoxy and the testing contacts. In the cells without oxygen, instead of seeing simply an increase in P3HT response, the P3HT response remains about the same but the dye response completely vanishes. Thus, the expected energy transfer pathway is not observed. Rather, the P3HT may be completely bypassing the dye somehow in the solar cell process, fulfilling the functions of light-absorber, hole-transporter, and charge-injector.



b) Sealed in glovebox under N₂

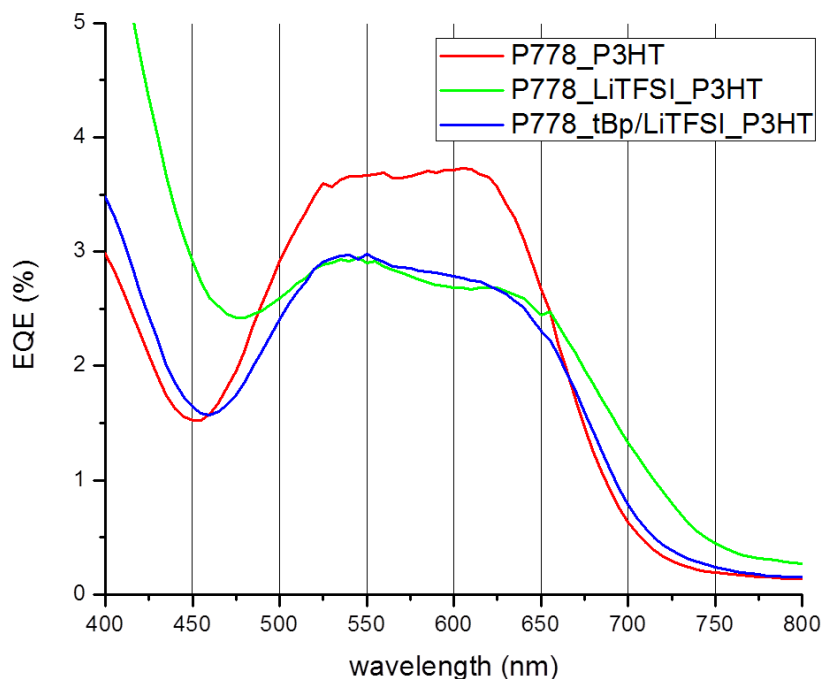


Figure 8. a) Spectral response of a P778/P3HT device with different additives fabricated and sealed in air; b) spectral response of a P778/P3HT device with different additives fabricated and sealed in the glovebox under an N₂ atmosphere.

Conclusion

Numerous experiments have been designed and carried out to test the effects of additives and the effects of atmospheric oxygen on the conducting polymer hole-transporter, P3HT. Tests of additives in devices have confirmed expectations taken from the literature, and in some cases optimal concentrations have been determined. Results from sealing tests indicate that the energy transfer mechanism expected from P3HT to an acceptor dye may be more complex than it seems. More robust experiments must be carried out with explicit care taken to define what exactly is being measured. In addition, as only a few dyes have been incorporated into P3HT solid-state dye-sensitized devices, many more near-infrared dyes must be synthesized and tested to make significant progress towards achieving widespread cheap, solution-processable solar energy conversion technology.

References

1. Nocera, D. G. "Fast Food" Energy. *Energy Environ. Sci.* **2010**, *3*, 993-995.
<http://web.mit.edu/5.03/www/notes/energy_molecules/fast_food.pdf>.
2. "EIA – 2010 International Energy Outlook - World Energy Demand and Economic Outlook." U.S. Energy Information Administration. July 27, 2010.
<<http://205.254.135.24/oiaf/ieo/world.html>>.
3. Hagfeldt, A.; Boschloo, G.; Sun, L.; Kloo, L.; Pettersson, H. "Dye-Sensitized Solar Cells." *Chem. Rev.* **2010**, *110*, 6595–6663.
4. "Solar Energy Data from World on the Edge." Earth Policy Institute. January 12, 2011.
<http://www.earth-policy.org/datacenter/pdf/book_wote_energy_solar.pdf>.
5. O'Brien, Chris. "Why Less is More: How Thin-film Manufacturing is Finding Momentum." Photovoltaics World. February 7, 2011.
<<http://www.renewableenergyworld.com/rea/news/article/2011/02/why-less-is-more-how-thin-film-manufacturing-is-finding-momentum>>.
6. Grätzel, M. "The Advent of Mesoscopic Injection Solar Cells." *Prog. Photovoltaics* **2006**, *14*, 429.
7. Anscombe, N. "Solar cells that mimic plants." *Nature Photonics.* **2011**, *5*, 266-267.
8. "Titanium Dioxide (TiO₂) Uses and Market Data." ICIS.com. July 2010.
<<http://www.icis.com/v2/chemicals/9076546/titanium-dioxide/uses.html>>.
9. Snaith, H. J.; Schmidt-Mende, L. "Advances in Liquid-Electrolyte and Solid-State Dye-Sensitized Solar Cells." *Adv. Mater.* **2007**, *19*, 3187–3200.